Measurement of Local Viscoelasticity and Forces in Living Cells by Magnetic Tweezers

Andreas R. Bausch,* Winfried Möller,† and Erich Sackmann*
*Physik Department E22 (Biophysics group), Technische Universität München, D-85748 Garching; and †GSF-Forschungszentrum für Umwelt und Gesundheit, Klinische Kooperationsgruppe "Aerosolmedizin" des Instituts für Inhalationsbiologie, D-82131 Gauting, Germany

ABSTRACT We measured the viscoelastic properties of the cytoplasm of J774 macrophages with a recently developed microrheometer. Ferromagnetic beads (1.3 μm in diameter) were used to determine the local viscoelastic moduli. Step-force pulses were applied to the magnetic beads and the displacement was observed by single particle tracking. By analyzing the creep response curves in terms of a triphasic mechanical equivalent circuit, we measured the shear elastic modulus, the effective viscosities, and the strain relaxation time. The values of the shear modulus vary by more than an order of magnitude within the cell population (range, 20–735 Pa; average, 343 Pa) and by a factor of 2 within single cells. The effective viscosity of the cytoplasm exhibits a relatively sharp distribution about an average of $\eta = 210$ Pa s ($\pm$ 143 Pa s). We measured the displacement field generated by the local forces by observing the induced motion of nonmagnetic beads. Even at distances of the order of 1 μm, no induced motion was seen, suggesting that the cytoplasm is composed of clusters of densely packed and cross-linked filaments separated by soft regions. In another series of experiments we analyzed the magnetophoretic motion of the ferromagnetic beads at a constant magnetic force. Measuring the bead velocity parallel and perpendicular to the applied force showed that local active forces on the beads varied from 50 to 900 pN.

INTRODUCTION

The viscoelasticity of the cytoplasm is a crucial physical parameter for many cellular processes such as intracellular transport of vesicles or other intracellular compartments and cell locomotion. However, measurement of this important property is hampered by the high degree of heterogeneity of the cell cytoplasm and the large forces (of the order of nano-Newton) required to measure viscoelastic moduli. One promising technique is microrheology by magnetic beads, pioneered 40 years ago (Amblard et al., 1996; Crick and Hughes, 1949; Ziemann et al., 1994). Because of technical difficulties in generating high local magnetic fields and field gradients and the lack of spherical magnetic beads, quantitative measurements were possible only with large beads ($\sim$10 μm in diameter) and in large cells such as sea urchin eggs (Hiramoto, 1969a,b).

Viscoelastic properties of smaller cells (such as macrophages) were measured by torsional deformations inside cells achieved by magnetic twisting of magnetic beads (Valberg and Butler, 1987; Valberg and Feldman, 1987; Möller et al., 1997). With this technique, apparent viscosities of the cytoplasm were measured and a nonlinear viscoelastic behavior was reported.

Until now, there have been only a few attempts to measure the forces exerted inside moving cells, so these forces remain unknown. Guilford et al. (1995) were the first to measure internal forces directly. They used magnetic beads with a diameter >6 μm that had been phagocytized by macrophages.

We recently developed a magnetic bead microrheometer capable of generating forces in the nano-Newton range on superparamagnetic and ferromagnetic beads with diameters smaller than 5 μm. By analyzing the deflection of the beads using particle tracking techniques, viscoelastic response and recovery curves can be measured with a spatial resolution of 10 nm and a time resolution of $t = 0.04$ s. This technique was recently applied to measure the viscoelastic moduli of plasma membranes of fibroblasts (Bausch et al., 1998). Compared to other techniques that allow local measurements of viscoelasticity from the outside (Daily et al., 1984; Radmacher et al., 1996), the technique presented here allows local measurements both inside and outside single cells.

In this paper we report, first, local measurements of viscoelastic moduli of the cytoplasm of macrophages by viscoelastic creep experiments using ferromagnetic beads with a diameter of 1.3 μm. Second, we present attempts to measure the displacement field generated by local forces following Bausch et al. (1998), by observation of the induced motion of nonmagnetic colloidal probes. In contrast to the postulation of transgressing elastic fields in cells (Maniotis et al., 1997), we did not find appreciable long-range elastic coupling within the cells. In a third type of experiment we showed that by analyzing the magnetophoretic motion of the beads subjected to a constant magnetic force, local active forces generated in the cytoplasm can be measured.

MATERIALS AND METHODS

The magnetic tweezers setup

The experimental setup of the microrheometer has been described previously by Bausch et al. (1998). It consists of a central measuring unit

Received for publication 31 March 1998 and in final form 12 September 1998.

Address reprint requests to Dr. Andreas R. Bausch, Technische Universität München, Lehrstuhl für Biophysik E22, James-Franck-Strasse, D-85748 Garching, Germany. Tel.: +49 (089) 289-12478, Fax: +49 (089) 289-12469; E-mail: abausch@physik.tu-muenchen.de.

0006-3495/99/01/573/07 $2.00

(including a sample holder and one magnetic coil with 1200 turns of 0.7-mm copper wire) mounted on an AXIOVERT 10 microscope (Zeiss, Oberkochen, Germany). The coil current was produced by a voltage-controlled current supply that transforms the voltage signal of a function generator FG 9000 (ELV, Leer, Germany) into a current signal with amplitudes up to 4 A. The microscope image was recorded by a CCD camera (C3077, Hamamatsu Photonics, Hamamatsu City, Japan) connected to a videorecorder (WJ-MX30, Panasonic, Osaka, Japan). The recorded sequences were digitized using an Apple Power Macintosh 9500 (Apple Computer, Cupertino, CA) equipped with a LG3 frame grabber card (Scion Corp., Frederick, MD). The position of the magnetic beads was determined with an accuracy of about 10 nm using a self-written single-particle tracking algorithm implemented with National Institutes of Health Image public domain image-processing software (NIH, Bethesda, MD). The time resolution as determined by the videofrequency was 0.04 s.

Sample preparation

All measurements were made with J774 mouse macrophages (European Collection of Animal Cell Cultures, Salisbury, UK). The cells were cultivated in an incubator at 37°C and 5% CO_2. The cell culture medium consisted of HEPES buffered RPMI 1640 with 5% v/v fetal calf serum (both from Life Technologies GmbH, Eggenstein, Germany). Cells were trypsinized every 4 days. Before each experiment the cells were transferred after trypsination from the culture dish onto uncoated cover glasses. The beads were dispersed in culture medium, which was then added to the already adherent cell preparation 2 days before the measurements in order to allow complete phagocytosis by the macrophages.

Monodispersed ferromagnetic beads with a diameter of 1.3 μm were prepared as described in Möller et al. (1990). Carboxylated latex beads with a diameter of 2 μm or melamin-coated beads with a diameter of 1 μm (Polybeads, Polisciences, Warrington, PA) were used as nonmagnetic colloidal probes. All measurements were performed in culture medium at 37°C.

Force calibration of the setup

To calibrate the distance dependence of the force acting on the magnetic bead, the bead velocity was determined near the magnetic pole piece in liquids of known viscosity at different coil currents ranging from 250 to 2500 mA as described by Bausch et al. (1998). The bead velocity was computed from the measured displacement-time graphs by numerical differentiation. Fig. 1 shows the results of a typical calibration of the force on a 1.3-μm ferromagnetic bead. For these calibration measurements we used dimethyl-polysiloxane with a kinematic viscosity of 12,500 cSt (Sigma, St. Louis, MO) as a calibrating liquid.

The velocity curves were converted into force curves using Stokes' law. In Fig. 1 *a*, the force is plotted versus the distance to the pole piece for various coil currents. For the highest coil currents, forces of up to 3000 pN on a 1.3-μm ferromagnetic bead were reached. The curves shown in Fig. 1 *a* were determined by using the same bead, which was aspirated by a micropipette after each measurement and pulled back to its starting position located 110 μm from the tip of the pole piece. In Fig. 1 *b*, the force is plotted as a function of the coil current and for various distances of the bead from the tip of the pole piece.

The net error of the absolute force calibration is determined by the standard deviations of the bead size and from calibration measurements. It can be estimated to be 15–20%.

Creep experiments and data evaluation

Creep experiments were performed by recording the deflection and recovery of the magnetic bead following sequences of rectangular force pulses. Typical trajectories of the beads are shown in Fig. 2 *a*. The creep response curves consisted of three regimes: a very fast elastic response, a slowing down of the deflection, and a viscous flow. The last regime is also characterized by the fact that the beads do not relax completely. It is convenient and customary to describe such triphasic behavior in terms of the mechanical equivalent circuit of Fig. 3, which consists of a Kelvin (or Zener) body in series with a dashpot η_0. Following Bausch et al. (1998), the creep compliance of the equivalent circuit is

$$J(t) = \frac{1}{\mu_0}\left(1 - \frac{\mu_1}{\mu_0 + \mu_1} \cdot e^{-t/\tau}\right) + \frac{t}{\eta_0} \qquad (1)$$

where the first term on the right side accounts for the Kelvin body and the second describes the viscous flow regime. The relaxation time is given by

$$\tau = \frac{\eta_1(\mu_0 + \mu_1)}{\mu_0\mu_1} \qquad (2)$$

As shown in detail in a previous study on in vitro models of actin networks, the linear deflection of the bead in the direction of the force $x(t)$ can be related to the force $f(t)$ by a simple (approximate) relationship:

$$gx(t) = J(t)\,f(t)$$

where $J(t)$ is the creep compliance and g is a geometric factor of the dimension of length. We assume that the same geometric parameter holds approximately for the cytoplasm because the bead diameter is small in relation to the cell dimension. Furthermore, as will be argued below, we can describe J in terms of friction of a bead in an isotropic and infinite

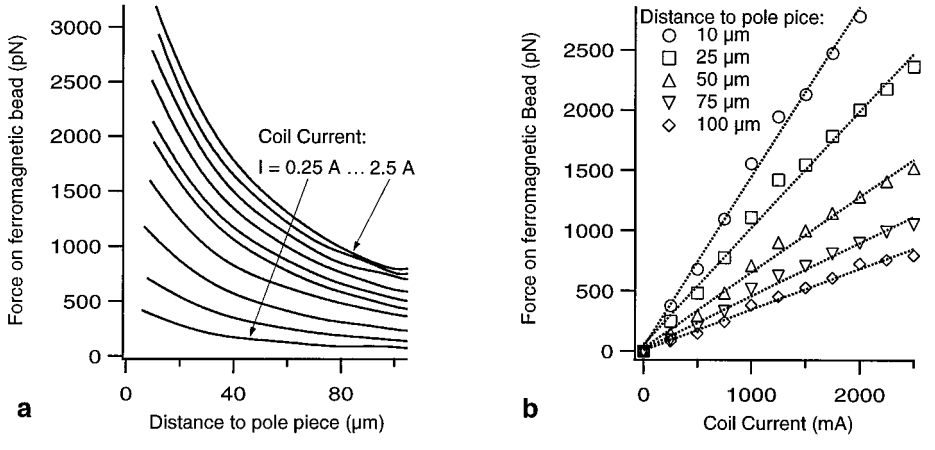

FIGURE 1 Force calibration of a ferromagnetic bead with a diameter of 1.3 μm. (*a*) Distance dependence of the force on the bead for 10 different coil currents (range, 250-2500 mA). (*b*) Force-versus-current curves for five distances showing a linear relationship between the coil current and the force on the ferromagnetic bead.

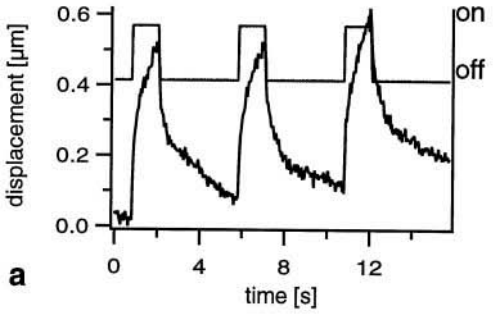

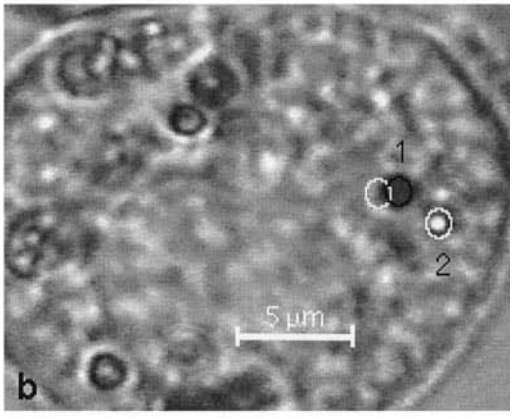

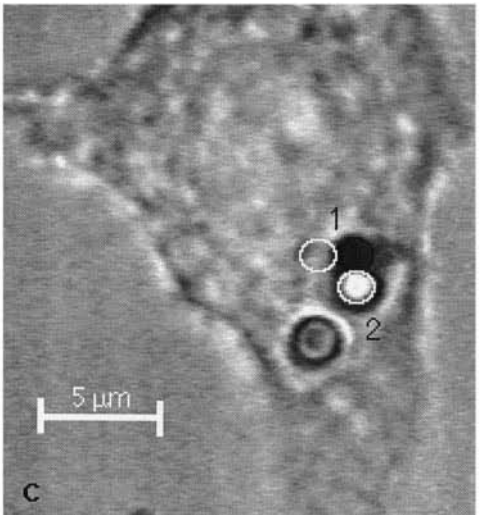

FIGURE 2 (*a*) Typical creep response and recovery curve of 1.3-μm diameter magnetic bead embedded in cytoplasm of the cell shown in (*b*). Force pulses of $f = 400$ pN and $t = 1.3$ s duration were applied. The viscoelastic response consisted of a fast elastic regime, a slowing down of the displacement, and a viscous flow. The last phase resulted in a residual deflection after switching off the field. (*b*) Phase contrast micrograph of macrophage with internalized magnetic (1) and latex (2) beads. Black circles indicate initial position of bead and white circles its position after a force pulse. Note that the latex bead does not show any displacement. The distance between the centers of the magnetic and latex beads is 2.4 μm. (*c*) Demonstration of the extreme short-range behavior of the deformation field. Black circles indicate initial position of bead; white circles indicate the position after a force pulse. Note that the large deflection of the magnetic bead (1) is a consequence of the fact that it consists of two attached beads of a diameter of 1.3 μm. Black circles indicate initial position; white circles indicate position after a force pulse.

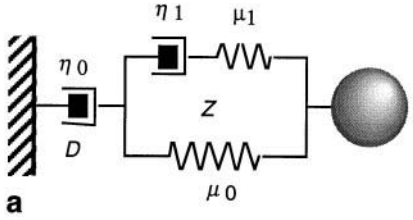

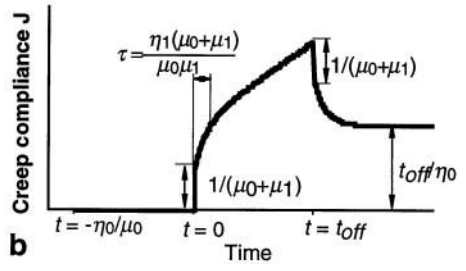

FIGURE 3 Mechanical equivalent circuit enabling formal representation of creep response and recovery curves. (*a*) Mechanical model consisting of a Kelvin (or Zener) body (Z) and a dashpot (D) in series. (*b*) Theoretical creep response and recovery curve of the mechanical equivalent circuit exhibiting the three experimentally observed regimes of response.

medium. For an infinite viscoelastic medium, $g = 6\pi a$, where a is the bead radius (Ziemann et al., 1994).

The four viscoelastic parameters, μ_0, μ_1, η_0, and η_1, are obtained by fitting Eq. 1 to the observed creep response curves. As shown in the examples of Fig. 4, a good agreement between experimental and theoretical creep response and recovery curves is achieved.

RESULTS

Measurement of local viscoelastic parameters

The four viscoelastic parameters required to account for the creep response and recovery curves were measured in eight different cells by application of different forces. In each experiment a series of field pulses was applied. The force amplitudes were varied from 277 to 686 pN and pulse duration times varied from 1 to 5 s. In general, sequences consisting of 4 pulses were analyzed. The series of field pulses yielded almost identical response curves. By fitting the recovery curves, similar values were found. In a few cases, forces as high as 1 nN were not sufficient to displace the bead. Within the range of forces applied, the values of the viscoelastic parameters did not vary remarkably with force amplitude and no strain hardening was observed. This indicates that the cytoplasm behaves as a Newtonian liquid. Moreover, the duration of the pulses had no influence on the obtained viscoelastic parameters. Only at pulse durations longer than 10 s could a hardening be observed, as can be seen below in Fig. 7.

In Fig. 5, the measured parameters η_o, $\mu = \mu_0 + \mu_1$, and $\tau = \eta_1\ \mu/\mu_0\ \mu_1$ are presented. In order to show the variability of the viscoelastic parameters within one cell and from cell to cell, the data obtained in the 12 experiments in 8 different cells are presented. The values measured in the

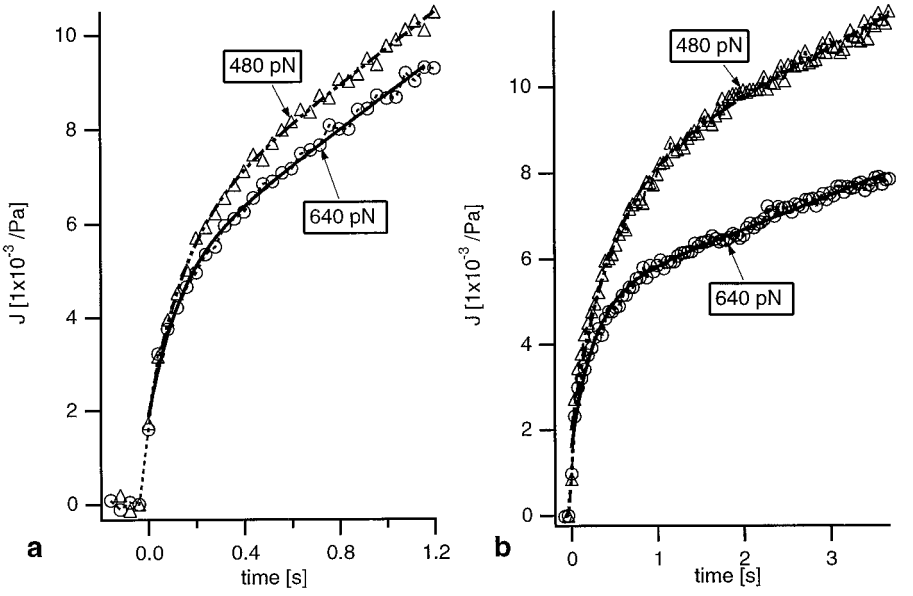

FIGURE 4 : Examples of analysis of the creep response curves (*left*) and recovery curves (*right*) in terms of equivalent circuit of Fig. 3. In each image the circles represent the experimental data for force pulses of f_m = 480 pN and f_m = 640 pN, respectively, and the drawn curves are optimal fits of Eq. 1 to the measured data.

same cell but at different positions and for different forces are characterized by the same symbol.

Fig. 5 shows the variability of the measured viscoelastic parameters. We found a relatively sharp distribution of the effective viscosity η_0, with the exception of one value. The same held for the relaxation time τ, again with only one exception. In contrast, the shear constant μ varied by more than one order of magnitude between different cells and by nearly a factor of 2 within one cell. We did not find a systematic difference between the viscoelastic parameters measured near the surface of the cell and those measured near its center.

In separate experiments we attempted to measure the spatial range of the elastic displacement field by observing the induced motion of nonmagnetic colloidal probes embedded into the cytoplasm together with the magnetic bead (Fig. 2, *b* and *c*). As nonmagnetic probes we used latex beads 1 μm or 2 μm in diameter. We barely observed an induced motion, even if the probe beads were located only ~1 μm from the magnetic bead, showing that the elastic

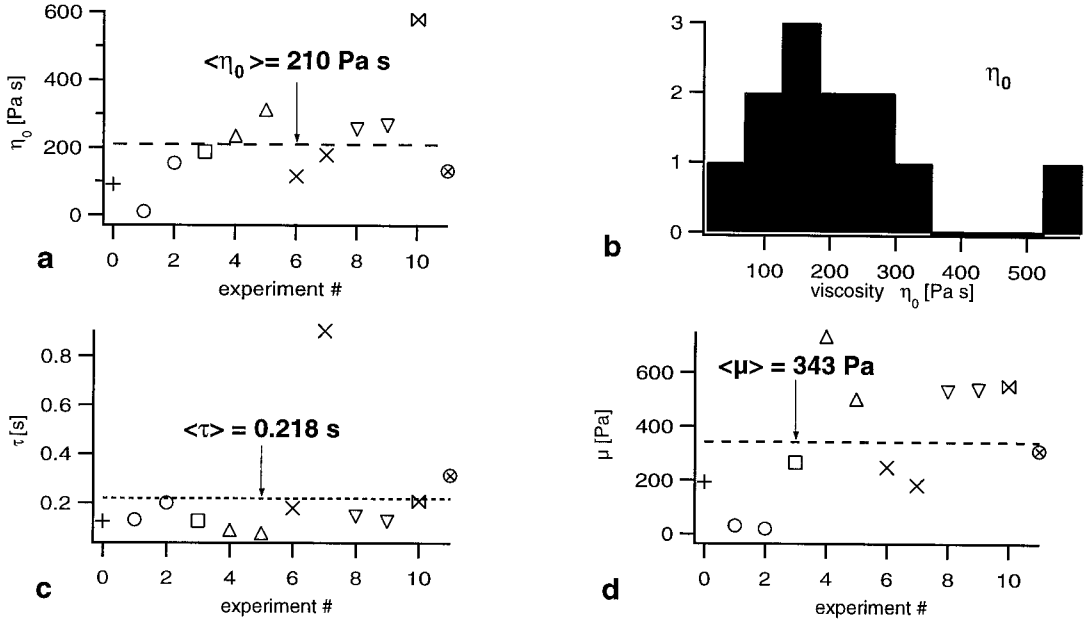

FIGURE 5 Summary of measured viscoelastic parameters. The values characterized by identical symbols correspond to the same cell but different forces. Each value was obtained by averaging over at least four creep response curves. (*a*) Summary of friction coefficients η_0 measured in experiments numbered 0 to 11. (*b*) Histogram of the dynamic viscosity η_0. (*c*) Values of measured relaxation times. (*d*) Summary of values of the total shear elastic constant $\mu = \mu_0 + \mu_1$.

field decays rapidly and that the cytoplasm does not behave as a continuous elastic medium.

Measurement of local active forces in the cytoplasm through magnetophoresis of colloidal beads

Occasionally the response curves were drastically distorted. We attributed this to the effect of local active forces in the cytoplasm. Especially in the direction perpendicular to the applied force, irregular movements were observable.

The mechanism of the directed transport of vesicles and intracellular compartments in cells is still largely unknown. It may occur through passive diffusion along concentration gradients or, more probably, the intracellular bodies could be actively transported along microtubili or actin cables, provided they exhibit motor proteins on the surface.

Local intracellular transport can be studied by observing the motion of intracellular compartments such as mitochondria or small particles (Janson et al., 1996; Ragsdale et al., 1997). However, this method does not yield information on intracellular forces.

A promising way to measure local forces is presented below. It is based on analysis of the motion of magnetic colloidal beads subjected to a constant magnetic force, which allows simultaneous measurements of the local viscosities and local forces.

In these magnetophoretic experiments step-like pulses of constant force and durations of up to 60 s are applied, resulting in the motion of the bead through nearly the whole cell in the direction of the applied force. A typical magnetophoretic trajectory in the image plane is shown in Fig. 6. It clearly exhibits large deflections in the direction normal to the average direction determined by the external force, which is defined as x-direction). The velocity in the y-direction, δv_y, is often larger than the local average velocity $\langle v_x \rangle$ in the x-direction (see Fig. 7 *c*) and is therefore attributed to active forces. Deviations of the bead motion from the x-direction by local obstacles (e.g., cellular compartments) would lead to $\delta v_y > \langle v_x \rangle$ and fluctuation in the velocity due to Brownian motion would be smaller than 10^{-9} m/s (because the diffusion constant $D \sim 1 \cdot 10^{-18}$ m^2/s for $\eta_0 = 200$ Pa s).

Because we are in the limit of small Reynolds numbers, the local velocity

$$\vec{v} = \langle \vec{v}_x \rangle + \delta\vec{v}$$

is determined by

$$6\pi\eta_{loc} a\vec{v} = \vec{f}_m + \vec{f}_{act}$$

where $\vec{f}_m$ is the known magnetic force and $\vec{f}_{act}$ the unknown local active force. The active force can be measured provided η_0 is known. Because the locally measured η_0 exhibits a relatively sharp distribution (cf. Fig. 5), it is expected to change only smoothly within the cell and can thus be obtained by measuring the average velocity over a time

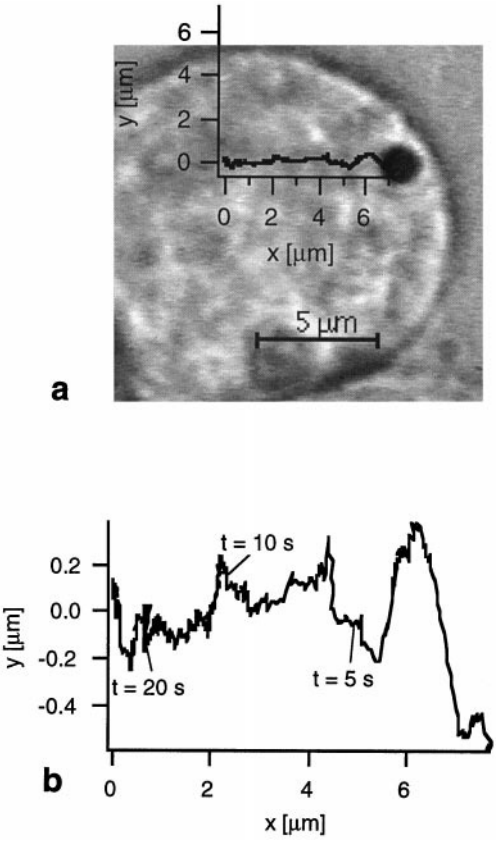

FIGURE 6 a) Trajectory of a magnetic bead in a macrophage subjected to a magnetic force $\vec{f}_m$ in the x-direction. (*a*) The large fluctuations of the bead in the direction perpendicular to the force direction (denoted as y) are attributed to active motions. The motion is thus decomposed into a constant motion with average velocity $\langle v_x \rangle$ due to magnetic force and a component generated by an active force f_{act}. (*b*) Enlarged view of the motion.

scale of about 10 s. From $\langle v_x \rangle = f_m/6\pi\eta_{loc}\, a$, the active force is obtained according to

$$\vec{f}_{act} = |\vec{f}_m| \frac{\vec{\delta v}}{|\langle v_x \rangle|}.$$

Fig. 7 *c* presents histograms of the velocity fluctuation for the example given in Fig. 6. In Fig. 7 *b* some values of the forces are indicated showing that they vary from 50 to 360 pN in this example. In other experiments forces of up to 900 pN were measured.

Because the beads were displaced by > 2 μm, the plane of focus of the bead position changed slightly and had to be readjusted. Because velocity fluctuations were analyzed only in the image plane, the actual forces are expected to be generally larger.

DISCUSSION

The main purpose of the present work was to show that magnetic bead microrheology is a valuable tool for charac-

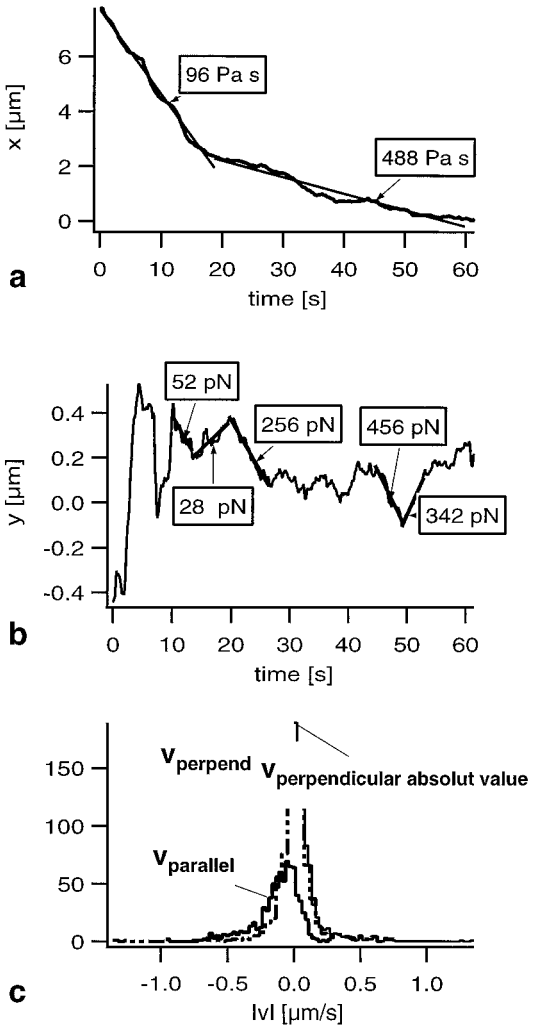

FIGURE 7 Analysis of the magnetophoretic motion of a bead. The motion in the image plane is decomposed into components parallel (*a*) and perpendicular (*b*) to the direction of the magnetic force. The local average viscosity is obtained according to $\eta = f_m/6\pi a\langle v_x\rangle$. (*a*) We assume two slopes to fit *x*-*t* curves. The velocity fluctuation δv_y in the *y*-direction are obtained from local linear fits of the *y* versus *t* curves, as indicated by the bold lines. The local active forces were calculated according to $\vec{f}_{act} = \vec{f}_m(\vec{\delta v}/\langle v_x\rangle)$ and some values are indicated at the trajectories (*b*). (*c*) Histogram of velocities in the directions parallel and perpendicular to the direction of the magnetic force.

terizing the structure of the cytoplasm of single cells quantitatively (by local measurement of viscoelastic parameters) and measuring local driving forces of cytoplasmatic transport.

The creep response curves consist of a fast elastic deflection of the bead, a slowing down of the displacement, and a viscous flow. The triphasic behavior is formally accounted for by the equivalent circuit shown in Fig. 3, comprising four elements. The amplitude of the elastic displacement is determined by the sum of the elastic moduli, $\delta x \sim f_{magn}/(\mu_1 + \mu_0)$. The denominator is thus a measure for the local shear modulus of the cytoskeleton. The dashpot η_1 and the spring μ_1 essentially determine the relaxation time $\tau = \eta_1(\mu_1 + \mu_0)/\mu_1\mu_0$, which is a measure of the time after which the elastic stress exerted by the network surrounding the bead relaxes. The dashpot η_0 characterizes the effective viscosity of the cytoplasm.

In about 10% of cases the creep curves exhibit a direct crossover from the elastic into the flow regime or the amplitudes may be strongly enlarged or diminished. These large fluctuations may occur within one series of pulse sequences and are attributed to the active forces. However, as the technique pioneers a new field of investigation, no detailed understanding of these processes is yet possible.

In order to gain insight into the range of spatial connectivity of the cytoplasmic networks, we embedded nonmagnetic colloidal beads and observed the motion of the beads induced by the deflection of the magnetic bead. Surprisingly, no induced deflection was generally observed, even if the magnetic and probe beads were separated by only about 1 μm. This behavior has been found near the rim and near the center of the cell. If the cytoplasm behaved as a homogeneous elastic continuum, the deformation field should scale as $u \approx F/(\mu^* d)$ (Landau and Lifshitz, 1959). A deflection of the magnetic bead of 500 nm should yield a deformation of 250 nm at a distance of 1 μm. Such a deformation could easily be observed by our technique.

These results provide some evidence that the whole cytoskeleton is composed of clusters of densely packed and/or strongly cross-linked filaments (actin, tubulin, and intermediate filaments) separated by very soft or sol-like regions. The formation of such heterogeneous networks, called microgel states, has been observed in, for instance, in vitro models of actin networks. At high cross-linker-to-actin ratios, the network decomposes into domains of densely packed and strongly cross-linked actin filaments separated by regions of low polymer density. These so-called percolated networks exhibit a large macroscopic elastic moduli (Tempel et al., 1996), whereas the local stiffness may fluctuate by at least one order of magnitude (F. G. Schmidt and E. Sackmann, unpublished results). A small local deflection of approximately 1 μm amplitude in such a microgel is expected to decay rapidly at the surface of the cluster, resulting in a weak elastic coupling between the clusters. This could provide an explanation for the rapid decay of the elastic field observed by our displacement field mapping experiments.

The heterogeneous elastic structure of the cytoplasm is also demonstrated by the large fluctuations of the shear elastic modulus, which varies by about a factor of 2 within a single cell and even more drastically (by an order of magnitude) from cell to cell. For μ we found values ranging from 20–735 Pa (average, 343 Pa) ($\mu_0 = 118 \pm 91$ and $\mu_1 = 225 \pm 143$). This behavior contrasts with the relatively sharp distribution of the local effective viscosity of the cytoplasm at about the value $\eta_0 \sim 210 \pm 140$ Pa s.

An interesting question concerns the recovery of the elastic strain. It could be due to the local flow of the filaments forming the network or to the breakage of local cross-links. In the latter case, $\mu = \mu_0 + \mu_1$ would be the yield stress of the local network rather than the elastic constant. At the technique's present stage of development we cannot distinguish between these two possibilities.

Our value of η_0 is remarkably larger than the value of 10 Pa s reported for sea urchin eggs (Hiramoto, 1969a,b) but considerably smaller than the value of 10^4 Pa s found for squid axon (Sato et al., 1984). Apparent viscosities were measured inside of lung macrophages by twisting magnetic bead yields (Valberg and Butler, 1987; Valberg and Feldman, 1987). At high shear rates of 0.05 1/s a value of 254 Pa s was found, whereas at 0.001 1/s the apparent viscosity was 2745 Pa s. The high shear rate yields viscosities comparable to ours, although the time scale is one order of magnitude longer than the one used in this study.

Because the magnetic beads are internalized by phagocytosis, they are expected to behave as phagosomes or lysosomes. As a consequence they are wrapped by a bilayer membrane that exhibits essentially the same composition of the outer membrane leaflet as other intracellular compartments. The magnetic beads are thus expected to mimic the behavior of the intracellular bodies. This holds, in particular, for the local forces exerted on the beads. Their origin is not clear yet. They could be generated by local cytoplasmic flow or by motor proteins incorporated into the beads' membrane envelope. To our knowledge this is the first time local fluctuating forces were measured. Until now, forces were measurable only by averaging during longer periods of time. Guilford et al. (1995) measured the average internal forces of moving pulmonary macrophages using a clever feedback control technique and magnetic beads 6 μm in diameter. They found that the macrophages exert forces in the range of 2–10 nN during locomotion.

Further studies will be necessary to understand the complex viscoelastic properties of the cell cytoplasm and the forces excerted inside cells. For a better understanding of cell locomotion, it is important to understand the correlations between local rheological properties and local force generation. Magnetic bead microrheology will be a valuable tool for exploring such correlations.

This work was supported by the Deutsche Forschungsgemeinschaft (Sa 246/22–3 and SFB413-C3) and the Fonds der Chemischen Industrie. We are particularly grateful to Joachim Rädler and Alexej Boulbitch for very helpful discussions.

REFERENCES

Amblard, F., B. Yurke, A. Pargellis, and S. Leibler. 1996. A magnetic manipulator for studying local rheology and micromechanical properties of biological systems. *Rev. Sci. Instr.* 87:818–827.

Bausch, A. R., F. Ziemann, A. A. Boulbitch, K. Jacobson, and E. Sackmann. 1998. Local measurements of viscoelastic parameters of adherent cell membranes by magnetic bead microrheometry. *Biophys. J.* 75: 2038–2049.

Crick, F. H. C., and A. F. W. Hughes. 1949. The physical properties of cytoplasm: a study by means of the magnetic particle method. *Exp. Cell Res.* 1:37–80.

Daily, B., E. L. Elson, and G. I. Zahalak. 1984. Cell poking: determination of the elastic area compressibility modulus of the erythrocyte membrane. *Biophys. J.* 45:661–682.

Guilford, W. H., R. C. Lantz, and R. W. Gore. 1995. Locomotive forces produced by single leukocytes in vivo and in vitro. *Am. J. Physiol.* 268:C1308–C1312.

Hiramoto, Y. 1969a. Mechanical properties of the protoplasm of the sea urchin egg. I. Unfertilized egg. *Exp. Cell Res.* 56:201–208.

Hiramoto, Y. 1969b. Mechanical properties of the protoplasm of the sea urchin egg. II. Fertilized egg. *Exp. Cell Res.* 56:209–218.

Janson, L. W., Ragsdale, K., and K. Luby Phelps. 1996. Mechanism and size cutoff for steric exclusion from actin-rich cytoplasmic domains, *Biophys. J.* 71:1228–1234.

Landau, L. D., and E. M. Lifshitz. 1959. Theory of Elasticity. Pergamon Press, Oxford.

Maniotis, A. J., C. S. Chen, and D. E. Ingber. 1997. Demonstration of mechanical connections between integrins, cytoskeletal filaments, and nucleoplasm that stabilize nuclear structure. *Proc. Natl. Acad. Sci. USA.* 94:849–854.

Möller, W., S. Takenaka, M. Rust, W. Stahlhofen, and J. Heyder. 1997. Probing mechanical properties of living cells by magnetopneumography. *J. Aerosol Med.* 10:173–186.

Möller, W., C. Roth, and W. Stahlhofen. 1990. Improved spinning top aerosol-generator for the production of high concentrated ferrimagnetic aerosols. *J. Aerosol Sci.* 21:S657–S660.

Radmacher, M., M. Fritz, C. M. Kacher, J. P. Cleveland, and P. K. Hansma. 1996. Measuring the viscoelastic properties of human platelets with the atomic force microscope. *Biophys. J.* 70:556–567.

Ragsdale, G. K., Phelps, J., and K. Luby-Phelps. 1997. Viscoelastic response of fibroblasts to tension transmitted through adherens junctions. *Biophys. J.* 73:2798–2808.

Sato, M., T. Z. Wong, D. T. Brown, and R. D. Allen. 1984. Rheological properties of living cytoplasm: a preliminary investigation of squid axoplasm (*Loligo pealei*). *Cell Motil.* 4:7–23.

Tempel, M., G. Isenberg, and E. Sackmann. 1996. Temperature-induced sol-gel transition and microgel formation in α-actinin cross linked actin networks: a rheological study. *Phys. Rev. E.* 54:1802–1810.

Valberg, P. A., and J. P. Butler. 1987. Magnetic particle motions within living cells. Physical theory and techniques. *Biophys. J.* 52:537–550.

Valberg, P. A., and H. A. Feldman. 1987. Magnetic particle motions within living cells. Measurement of cytoplasmic viscosity and motile activity. *Biophys. J.* 52:551–61.

Ziemann, F., J. Rädler, and E. Sackmann. 1994. Local measurements of viscoelastic moduli of entangled actin networks using an oscillating magnetic bead micro-rheometer. *Biophys. J.* 66:2210–2216.